Engineering 56 (2026) 79–86

Contents lists available at ScienceDirect

Engineering

journal homepage: www.elsevier.com/locate/eng

Research
6G: From Theory to Practice—Article

6G Space–Air–Ground Integrated Networks for Unmanned Operations: Closed-Loop Model and Task-Oriented Approach

Xinran Fang [a,b], Wei Feng [a,b,*], Yunfei Chen [c], Ning Ge [a,b], Shi Jin [d], Shiwen Mao [e]

[a] Department of Electronic Engineering, Tsinghua University, Beijing 100084, China
[b] State Key Laboratory of Space Network and Communications, Tsinghua University, Beijing 100084, China
[c] Department of Engineering, University of Durham, Durham DH1 3LE, UK
[d] National Mobile Communications Research Laboratory, Southeast University, Nanjing 210096, China
[e] Department of Electrical and Computer Engineering, Auburn University, Auburn, AL 36849, USA

ARTICLE INFO

Article history:
Received 28 November 2024
Revised 26 July 2025
Accepted 7 August 2025
Available online 26 August 2025

Keywords:
Radio map
Sensing–communication–computing–control (SC^3) loop
Space–air–ground integrated network
Sixth-generation (6G) communication
Task-oriented communication

ABSTRACT

In the upcoming sixth-generation (6G) era, supporting field robots for unmanned operations has emerged as an important application direction. To provide connectivity in remote areas, the space–air–ground integrated network (SAGIN) will play a crucial role in extending coverage. Through SAGIN connections, the sensors, edge platforms, and actuators form sensing–communication–computing–control (SC^3) loops that can automatically execute complex tasks without human intervention. Similar to the reflex arc, the SC^3 loop is an integrated structure that cannot be deconstructed. This necessitates a systematic approach that takes the SC^3 loop rather than the communication link as the basic unit of SAGINs. Given the resource limitations in remote areas, we propose a radio-map-based task-oriented framework that uses environmental and task-related information to enable task-matched service provision. We detail how the network collects and uses this information and present task-oriented scheduling schemes. In the case study, we use a control task as an example and validate the superiority of the task-oriented closed-loop optimization scheme over traditional communication schemes. Finally, we discuss open challenges and possible solutions for developing nerve system-like SAGINs.

© 2025 THE AUTHORS. Published by Elsevier LTD on behalf of Chinese Academy of Engineering and Higher Education Press Limited Company. This is an open access article under the CC BY-NC-ND license (http://creativecommons.org/licenses/by-nc-nd/4.0/).

1. Introduction

With the rapid development of sensing, communication, computing, and control, unmanned operations are expected to become a reality in the sixth-generation (6G) era. In particular, for applications in remote areas, such as oil and coal mining, disaster rescue, and scientific exploration, the demand for replacing humans with machines has become increasingly pressing [1]. With the Fukushima nuclear accident as an example, the presence of highly radioactive debris makes it dangerous for humans to access damaged reactors. Recently, Tokyo Electric Power Company Holdings revealed a "telesco-style" remote-controlled robot, which is undergoing test for retrieving melted debris. If successful, 880 tons of highly radioactive melted nuclear fuel can be properly disposed without sending humans to the scene [2].

Owing to geological limitations, ground-based platforms cannot be deployed in remote areas at a large scale. To enable 6G access anywhere, airborne and spaceborne platforms provide complementary coverage for ground-based infrastructure, leading to space–air–ground integrated networks (SAGINs) [3,4]. Within the SAGIN, different functional robots perceive, communicate, compute, and act in a coordinated manner. Specifically, they form a new structure named the sensing–communication–computing–control (SC^3) loop, where the sensor senses the environment and sends data to the edge platform, the edge platform performs data analysis and sends commands to the actuator, and the actuator takes action. With effective feedback, the SC^3 loop can adapt to varying environments and execute different tasks.

From a biological perspective, the SC^3 loop is similar to the reflex arc. The reflex arc consists of five components: the receptor, afferent nerve, nerve center, efferent nerve, and effector. Correspondingly, the SC^3 loop comprises the sensor, data-uploading link, edge center, command-downloading link, and actuator. In biology, ataxia is a rare disease, in which the reflex arc components remain

* Corresponding author.
E-mail address: fengwei@tsinghua.edu.cn (W. Feng).

https://doi.org/10.1016/j.eng.2025.08.025
2095-8099/© 2025 THE AUTHORS. Published by Elsevier LTD on behalf of Chinese Academy of Engineering and Higher Education Press Limited Company.
This is an open access article under the CC BY-NC-ND license (http://creativecommons.org/licenses/by-nc-nd/4.0/).

intact, yet movement is impaired because of dysfunction in the brain in integrating these parts [5]. Thus, the reflex arc cannot be activated with isolated, uncoordinated components. By analogy, the SC^3 loop is an integrated structure rather than a set of independent components. The five components must work in cooperation to execute complex tasks.

However, current communication systems focus only on bit-oriented links rather than the task-oriented SC^3 loop. For example, the fifth-generation (5G) system employs orthogonal frequency-division multiple access (OFDMA) to allocate resources across multiple users and uses time-division duplexing (TDD) or frequency-division duplexing (FDD) to separate uplink (UL) and downlink (DL) transmissions. While such a bit-oriented framework is effective for general-purpose connections, it overlooks the tight coupling among sensing, communication, computing, and control. The mismatch of different components leads to degraded system performance. In addition, current systems are predominantly modular. As a result, the communication layer is indifferent to the transmission environment and the served task. For the transmission environment, the communication layer relies on pilot-based estimation to estimate channel state information (CSI). With CSI only, the network cannot make precise, environment–aware decisions. For the served task, the task demands are mapped to quality-of-service (QoS) flows. Since QoS mapping accounts for the worst-case scenario among different factors, the communication layer has to provide excess supplies to guarantee the performance of upper-layer applications, thus limiting overall resource efficiency.

To address the resource limitations in remote areas, the 6G SAGIN should adopt an integrated, system-level approach, moving beyond the traditional deconstructed, modular design. We take the SC^3 loop—not the communication link—as the fundamental unit of the SAGIN. To shift from best-effort delivery to on-demand resource provisioning, we incorporate environmental and task-related information into the SAGIN design. Therefore, we propose a radio-map-based task-oriented framework that collects and utilizes extrinsic information to support intelligent decision-making. Building on this, we develop task-oriented closed-loop scheduling schemes that operates on two-time scales. In the case study, we use a control task as an example and validate the effectiveness of the proposed scheme. Finally, we outline open issues and discuss potential research directions to guide future work.

2. Typical applications and network structure

In Fig. 1, we illustrate the SC^3-loop-based 6G SAGIN and its typical applications. In our definition, the "task" refers to the application-level works that we apply the network to do. In the following, we choose oil and coal mining, disaster rescue, and scientific exploration as typical applications and analyze their common and unique communication demands.

2.1. Typical applications

Oil and coal mining: Due to the harsh environments, the mining industry is one of the earliest industries to use unmanned technology. With maritime oil drilling as an example, Equinor constructed the world's first fully automatic and remote-operated maritime oil platform, named the Oseberg H, in 2018, which reduces the oil production cost to less than 20 USD per barrel [6]. To enable remote operations, there is a proprietary fiber that connects the network on the platform and the offshore control center. During the drilling process, information for key rig operation parameters, such as rotational speed and displacement, is transmitted to the control center, where, artificial intelligence (AI)-enabled solutions such as Edrilling generate visualized three-dimensional (3D) models and provide guidelines for rig operations. To achieve precise control, hundreds of sensors are deployed on the oil platform, necessitating a gigabits-per-second (Gbps)-level UL data rate. Additionally, the cycle time of rig control is at the millisecond level, necessitating the development of transient computing models and ultralow-latency communication to fully support unmanned mining operations.

Disaster rescue: With advancements in manufacturing, many new rescue robots have been developed in recent decades. For example, Spot is an agile mobile robot that was invented by Boston Dynamics, USA. It can be used for cleaning sites after nuclear leakage and exposed to 82-year worth of the annual worker dose without failure [7]. In disaster rescue, timely response is highly important for saving lives and reducing losses. Since ground-based facilities are damaged during disasters, airborne platforms such as unmanned aerial vehicles (UAVs) and airships can be deployed quickly and provide communication, localization, and computing support for field robots [8]. It was reported that during the Ya'an earthquake, it took two and a half hours for the first rescue team to come to the scene, whereas if robots were used, this time could be reduced to tens of minutes. Once the SC^3 loops are established, minimizing the cycle time is critical for field robots to adapt to dynamic conditions. The reaction time of humans is approximately 0.2–0.3 s, which is still too long to avoid danger during emergencies. Therefore, the cycle time of the SC^3 loop must be at the millisecond level to ensure rapid and effective responses.

Scientific exploration: On Earth, only 26% of areas are suitable for humans to live, leaving vast areas that remain untouched by mankind. In addition, the outer space also waits for our exploration. In space exploration, robots usually form "mother–daughter system" [9]. With the planetary exploration as an example, the orbital carrier is a powerful mother robot. It carries daughter robots such as rovers, landers, and sensors, traveling from the Earth to the target planet. After reaching the predetermined orbit, the orbital carrier releases the daughter robots to the surface of the target planet. Then, it provides guidelines to the daughter robots. Since the planet conditions are unknown before landing daughter robots, the mother–daughter link is the lifeline for daughter robots. Real-time and reliable communication is highly important for daughter robots to address unforeseen circumstances. However, the energy limitations of space robots are a notable challenge for providing high-performance communication since small antenna arrays and low transmit power must be used.

We summarize the communication demands of these unmanned operations in Table 1 [10]. While all of them—oil and coal mining, disaster rescue, and scientific exploration—require wide-area coverage and low-latency communication, each also presents distinct and specialized demands. These diverse requirements reflect the limitations of one-size-fits-all communication and highlight the need for task-oriented design.

2.2. Network structure

As shown in Fig. 1, we illustrate the 6G SAGIN for unmanned operations. The network consists of ground-based, airborne, and spaceborne platforms. These platforms are assembled with communication transceivers, computing chips, and sensing modules as needed. They work at network edges to connect sensors and actuators to form SC^3 loops. In most cases, ground-based platforms are the main network devices, whereas airborne and spaceborne platforms are essential complementary means. They fill coverage gaps and share the responsibility of addressing overwhelming demands. In addition, there is a cloud center far from the field. The cloud center has powerful computing capabilities. It can be used to address complex situations that cannot be handled by edge platforms. Like the nervous system, the SAGIN is very complex. The

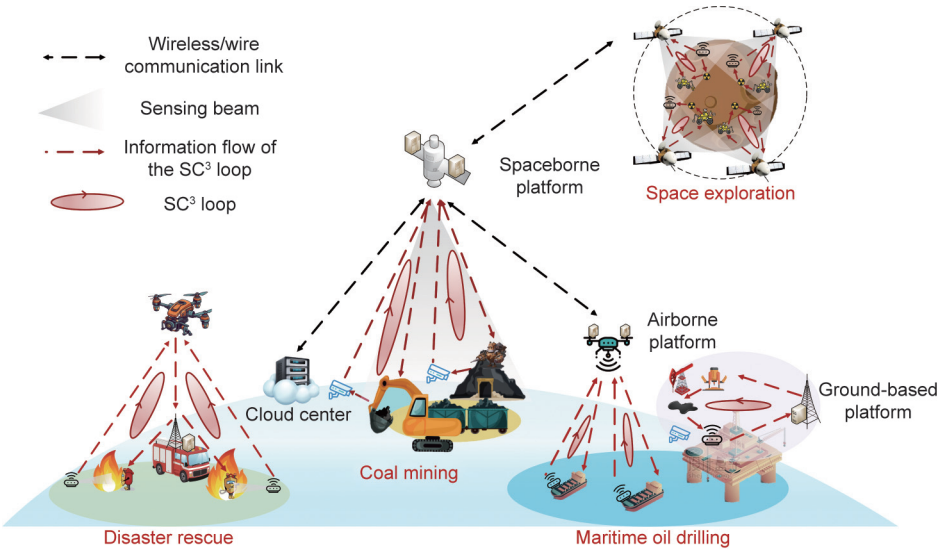

Fig. 1. Illustration of the 6G SAGIN for unmanned operations, such as disaster rescue, coal mining, maritime oil drilling, and space exploration. The network consists of spaceborne, airborne, and ground-based platforms. The basic unit of the SAGIN is an SC^3 loop.

Table 1
Communication demands of typical unmanned operations.

Applications	Latency	Coverage	Reliability	Energy	Unique traits
Oil and coal mining	Subsecond-level cycle time for controlling a mobile robot [10]	Tens of kilometers in underground and offshore environments	High	Adequate	High UL data rate for multi-sensor feedback
Disaster rescue	Subsecond-level cycle time for controlling a mobile robot [10]	Tens of kilometers to hundreds of kilometers in dispersed or inaccessible zones	Ultra-high	Limited	Low-latency response and adaptability to changing conditions
Scientific exploration	Subsecond-level cycle time for controlling a mobile robot [10]	Hundreds of kilometers in extreme conditions (i.e., polar regions and outer space)	Ultra-high	Ultra-limited	High reliability in extreme conditions

SC^3 loops are mutually coupled for sharing sensors, edge platforms, and actuators. In Fig. 2, we present the one-to-one correspondence between the reflex arc and the SC^3 loop. Specifically, the reflex arc components—the receptor, afferent nerve, nerve center, efferent nerve, and effector—align with the SC^3 loop elements: the sensor, data-uploading link, computing center, command-downloading link, and actuator. Furthermore, similar to the nervous system, which features a hierarchical structure comprising the spinal cord and brain, the computing center in the SAGIN is hierarchical, including both edge platforms and cloud centers. Building on these insights, we take the reflex arc-like SC^3 loop as the basic unit and explore the task-oriented closed-loop design.

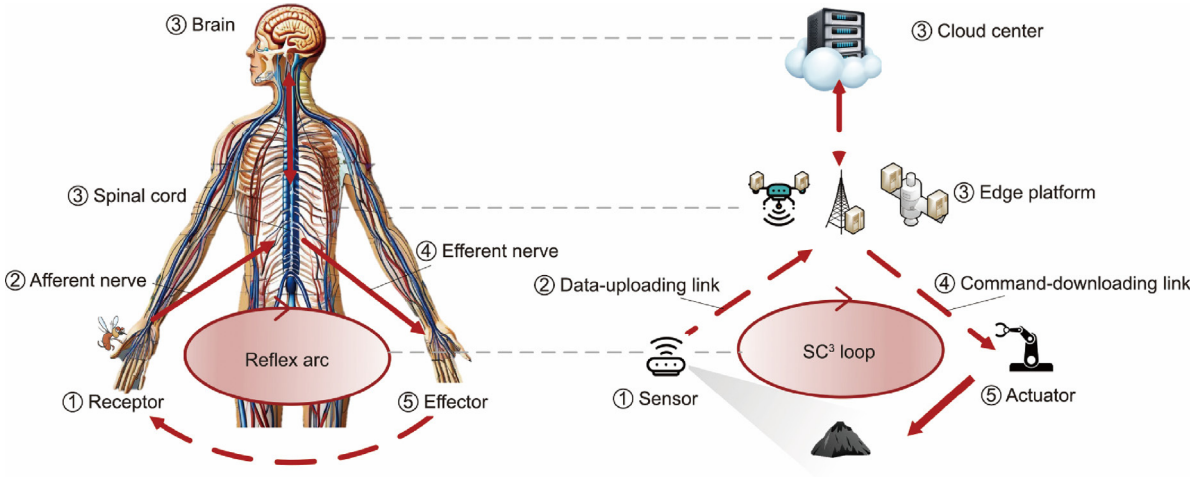

Fig. 2. Comparisons between the reflex arc and the SC^3 loop. There are interesting matchups between the five components of the reflex arc and the SC^3 loop: ① receptor and sensor, ② afferent nerve and data-uploading link, ③ nerve center (spinal cord and brain) and computing center (edge platform and cloud center), ④ efferent nerve and command-downloading link, and ⑤ effector and actuator.

3. Radio-map-based task-oriented framework

In this section, we propose our radio-map-based task-oriented framework. Unlike task-agnostic 5G systems, the proposed framework picks up environmental and task-related information and focuses on task performance behind data transmissions. This shift enables the SAGIN to provide task-matched services, which is particularly critical in remote scenarios. We illustrate our proposed framework in Fig. 3, where the radio map module is responsible for collecting environmental information and the task management module handles task-related information. With the information provided by these two modules, the scheduling center executes task-oriented closed-loop scheduling. In the following subsections, we detail each module and their specific functions.

3.1. Radio map module

The radio map module enables the network to "see" the environment. It consists of two units: a data management unit and a map estimation unit. The data management unit is used to collect and preprocess raw data, which includes semi-static data (e.g., terrains and building shapes) and dynamic data (e.g., real-time robot positions and spectrum activities). Since the raw data are naturally heterogeneous and noisy, they are usually unsuitable for direct resource scheduling. By applying tools such as machine learning models, the map estimation unit extracts high-level environmental information, such as large-scale CSI and predicted robot trajectories, from the raw data. This information is then sent to the scheduling center to support informed decision-making.

Although several studies have explored the use of radio maps [11], their practical deployment remains limited. In dynamic environments, radio maps may fail to promptly reflect environmental changes, providing inaccurate or outdated information. To improve robustness, real-time update techniques such as adaptive online learning and incremental map updates can be incorporated. Furthermore, a hybrid approach that combines machine learning-based predictions with traditional pilot-based estimations offers a practical solution. In this way, the system can leverage pilot-based estimations to correct radio-map predictions, thereby improving reliability and adaptability.

3.2. Task management module

The task management module enables the network to "see" the task. Since tasks are diverse in practice, we propose transforming the diverse task requirements into uniform loop metrics for general design. To achieve task-loop requirement mapping, AI-based models, such as digital twins, can be developed to simulate physical systems. According to the real-time simulation situations, the task management module learns the behavior of the system and determines the requirement for the SC^3 loop. To measure the SC^3 loop, entropy serves as a promising candidate to bridge connections among SC^3-loop components. The sensing, communication, computing, and control fields all involve entropy-based measurements, such as the estimation rate in sensing, the data rate in communication, the information bottleneck in computing, and the intrinsic entropy rate in control. Building on this insight, we introduce a new metric called the closed-loop negentropy rate (CNER). Analogous to the channel capacity, which measures the entropy reduction per channel use, CNER quantifies the entropy reduction per SC^3 cycle. It is a loop-level metric that integrates traditional entropy-based metrics of sensing, communication, computing, and control. Although improving individual QoS metrics—such as the data rate—can increase the CNER, it is not the most effective approach. This is because the SC^3 loop emphasizes intra-loop coordination rather than the isolated performance of individual functions. Serving as a systematic metric, CNER enables us to establish a task-oriented closed-loop optimization framework in which the SC^3 loop rather than a single communication link is selected as the basic unit. In addition to the information rate, the SC^3 loop can be measured from other perspectives, such as latency and reliability, and the corresponding loop-level metrics can be defined in a similar way as the CNER.

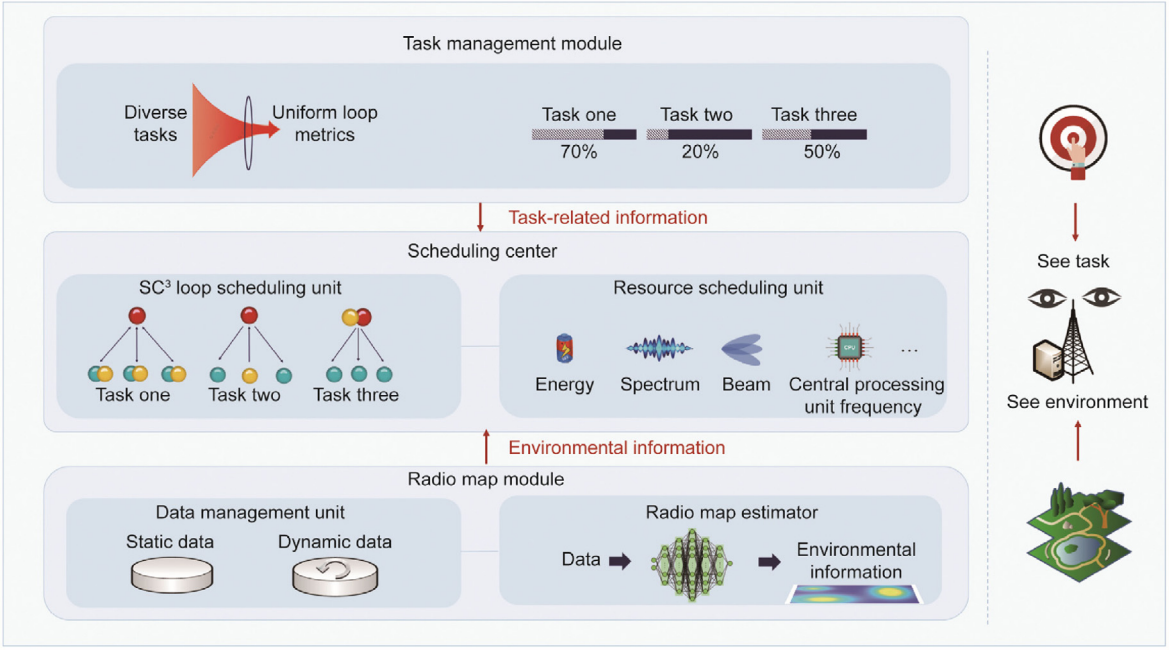

Fig. 3. Illustration of the radio-map-based task-oriented framework, which enables the network to "see" the environment and task. The yellow, red, and blue spheres in the SC^3 loop scheduling unit represent the sensing, computing, and control components, respectively.

The central challenge for the task management module lies in balancing the benefit and cost. While incorporating task-related information can enable task-matched resource provisions, it comes at the expense of increased design complexity. This complexity arises from the unknown relationships among task requirements, the performance of SC^3-loop components, and the overall performance of the SC^3 loop. Consequently, effectively mapping task requirements into network design remains an open problem. It is crucial to find a proper granularity to integrate task-level demands into network design. In many cases, a simple yet effective model may be better than a comprehensive one. With the control task as an example, complex nonlinear systems are often approximated as linear systems around their operating points and effectively regulated using a simple linear quadratic regulator (LQR). The control metric, represented by the LQR cost, has a clear closed-form relationship with the loop metric, the CNER [12]. This direct mapping enables control-oriented communication design. Owing to its simple yet effective trait, the LQR-based control has been widely applied in aerospace, industrial automation, and related fields.

3.3. Scheduling center

The scheduling center obtains environmental information from the radio map module and task-related information from the task management module. Accordingly, resources are scheduled to meet task requirements. The scheduling process is divided into two-time scales according to the scheduling granularity. The SC^3 loop scheduling unit takes charge of forming and dismissing SC^3 loops during the task execution process. To ensure the stable evolution of the network pattern, this scheduling is executed at a middle-time scale (e.g., the order of minutes or hours). The resource scheduling unit is responsible for scheduling fine-grained resources, such as spectrum, power, and central processing unit (CPU) frequency. To adapt to varying environments, these resources are adjusted in each SC^3 cycle (e.g., the order of seconds or subseconds). In the next section, we detail the corresponding scheduling schemes.

4. Task-oriented closed-loop scheduling

In this section, we detail how environmental and task-related information is used for informed decision-making. Although joint sensing, communication, computing, and control optimization strategies were proposed in previous studies, focus was typically placed on resource-level coordination, treating each function as an independent module. In contrast, we consider the task-level connections among the SC^3 loop components. Our scheduling schemes are designed by treating the SC^3 loop as an integrated structure, with the primary objective of maximizing task efficiency.

4.1. SC^3-loop scheduling

The SC^3-loop scheduling scheme is designed to form and dismiss SC^3 loops during the task execution process. To ensure the steady evolution of network patterns, SC^3 loops are scheduled at a middle-time scale, between those of large-scale network deployment (e.g., site selection and base station (BS) deployment) and small-scale resource scheduling. When a task is generated, the SC^3-loop scheduling unit obtains task-related information, such as the required number of loops and loop requirements, from the task management module. Then, the task-loop assignments and sensor–actuator pairings are determined. For airborne platforms such as UAVs, the SC^3-loop scheduling unit also determines the site and trajectory planning, as well as backhaul connections. During task execution, SC^3 loops are dynamically formed and dissolved according to evolving task demands. To ensure seamless handoffs across space, air, and ground layers, resources and field devices are managed through a prediction-based, process-oriented approach. These scheduling decisions are guided by integrating real-time network conditions with predictive modeling. For example, robot trajectories predicted by the radio map allow the network to proactively designate appropriate handover edge platforms along the movement path. Similarly, by estimating the progression of task execution, the SC^3-loop scheduling unit can pre-allocate resources for newly formed SC^3 loops by using the resources associated with the loops whose tasks are nearing completion. Therefore, environmental and task awareness enables the proposed framework to maintain operational continuity in complex and rapidly changing scenarios.

4.2. Resource scheduling

Given the SC^3 loop patterns, the resource scheduling unit schedules fine-grained resources such as spectrum, power, and CPU frequency within and across SC^3 loops. In the task-oriented closed-loop optimization, the loop metric, such as the CNER, is selected as the objective, and the SC^3-loop cycle time and resource limitations are considered in the constraints. For a task performed by a single SC^3 loop, maximizing the loop metric is equivalent to maximizing task efficiency. For a task performed by multiple SC^3 loops, we can use a weighted summation, such as sum-log function and maximum–minimum function, to account for the impacts of each SC^3 loop on the final task and choose a proper one in practical engineering. During resource scheduling, the radio map provides site-specific large-scale CSI, which includes both channel quality information and causes of degradation, such as shadowing, long-distance transmissions, and interference. This allows the network to make environment–aware adaptations. For example, if the degradation is attributed to interference, the resource scheduling unit can reallocate spectrum resources on the basis of spectrum activities from the radio map. When spectrum sharing is unavoidable, large-scale CSI can be used for adaptive power control [13,14], which omits the need for the pilot-based CSI estimation. Moreover, the radio map facilitates prediction-based designs. For example, if a movable actuator is about to enter a shadowed region, the edge platform can proactively send guidelines in advance and close connections in the shadowed region to prevent ineffective communication.

5. Case study

In this section, we provide an example to demonstrate the superiority of the proposed task-oriented closed-loop scheme. As shown in Fig. 4, we consider a satellite–UAV system that executes a control task such as radioactive-level control. The UAV is multifunctional that carries communication and computing modules. In each SC^3 cycle, it receives sensing data from sensors, calculates commands, and sends commands to actuators to take action. Synergistically, the sensors, UAV, and actuators form multiple SC^3 loops. During the task execution process, the satellite provides tracking, telemetry, and control (TT&C) services for the UAV. It also relays important data between the UAV and the cloud center, allowing the system to deal with complex situations that cannot be handled by the UAV alone.

Given the integrity of the SC^3 loop, we treat each sensor and actuator pair as a virtual user; thus, the sensor–UAV link and the UAV–actuator link are the UL and DL of the virtual user, respectively. We utilize the traditional QoS metric, namely, the data rate, to calculate the volumes of UL and DL transmitted data in an SC^3 cycle, denoted as D^{u} and D^{d} (bits per SC^3 cycle), respectively. The

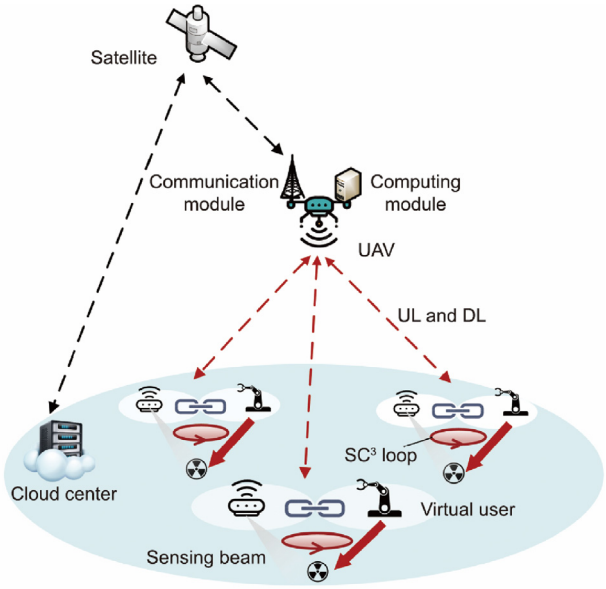

Fig. 4. Illustration of a satellite–UAV system that executes a control task. The UAV carries communication and computing modules, forming multiple SC^3 loops with the sensors and actuators. We regard each sensor–actuator pair as a virtual user. The sensor–UAV link and UAV–actuator link are the UL and DL of this virtual user, respectively.

computing process is modeled as an information extraction process in which the computing center extracts the task-related information from the UL transmitted data:

$$D^{\mathrm{u}} \to \rho D^{\mathrm{u}} \quad (0 < \rho < 1) \tag{1}$$

where ρ is the information extraction ratio. The computing time t^{c} is modeled as $t^{\mathrm{c}} = \frac{\alpha D^{\mathrm{u}}}{f}$, where α (CPU cycles per bit) is the required CPU frequency for processing one-bit information and f denotes the CPU frequency (Hz). The amount of information that finally works for the task—that is, the information received by the actuator in an SC^3 cycle, is determined by the bottleneck between the task-related information extracted from the data transmitted via the UL and the information transmitted via the DL:

$$D^{\mathrm{SC}^3} = \min\{\rho D^{\mathrm{u}},\ D^{\mathrm{d}}\} \tag{2}$$

where D^{SC^3} (bits per SC^3 cycle) is the CNER, which measures how much actionable and task-relevant information is closed through the SC^3 loop in each cycle. To quantitatively evaluate the proposed task-oriented closed-loop scheme against traditional communication-oriented schemes, we model the system under control as a linear time-invariant system of dimension m. The system state at time index t, $\boldsymbol{x}_t \in \mathbb{R}^{m\times 1}$ (where $\mathbb{R}$ is the set of real numbers), evolves according to the following equation:

$$\boldsymbol{x}_{t+1} = \boldsymbol{A}\boldsymbol{x}_t + \boldsymbol{B}\boldsymbol{u}_t + \boldsymbol{v}_t \tag{3}$$

where $\boldsymbol{A}$ denotes the system matrix, $\boldsymbol{B}$ denotes the input matrix, $\boldsymbol{u}_t$ denotes the control input, and $\boldsymbol{v}_t$ denotes the process noise with variance matrix $\boldsymbol{\Sigma}_{\boldsymbol{v}}$. The control performance of the SC^3 loop is evaluated using the LQR cost. A low LQR cost indicates effective control with few inputs, reflecting good control performance of the SC^3 loop. For a given time horizon N, the long-term LQR cost is computed as the mean accumulated penalty over N time steps. Accordingly, the infinite-horizon LQR cost is defined as:

$$l = \lim_{N\to\infty} \sup\ \mathbb{E}\left[\frac{1}{N}\sum_{t=1}^{N}\left(\boldsymbol{x}_t^{\mathrm{T}}\boldsymbol{Q}\boldsymbol{x}_t + \boldsymbol{u}_t^{\mathrm{T}}\boldsymbol{R}\boldsymbol{u}_t\right)\right] \tag{4}$$

where l denotes the LQR cost, $\boldsymbol{Q}$ and $\boldsymbol{R}$ are positive semidefinite weighting matrices that balance the penalty between state deviation and control effort, $\mathbb{E}[\cdot]$ represents the expectation operator. According to Ref. [11], the lower bound of the LQR cost is related to the CNER through a closed-form function,

$$l \geq \frac{mN(\boldsymbol{v})|\det \boldsymbol{M}|^{\frac{1}{m}}}{2^{\frac{2}{m}(D^{\mathrm{SC}^3} - \log_2|\det \boldsymbol{A}|)} - 1} + \mathrm{tr}(\boldsymbol{\Sigma}_{\boldsymbol{v}}\boldsymbol{S}) \tag{5}$$

where $N(\boldsymbol{v}) \triangleq \frac{1}{2\pi \mathrm{e}} \mathrm{e}^{\frac{2}{m}h(\boldsymbol{v})}$ with $h(\boldsymbol{v})$ denoting the differential entropy of $\boldsymbol{v}$, and $\boldsymbol{S}$ is the solution to the algebraic Riccati equation: $\boldsymbol{S} = \boldsymbol{Q} + \boldsymbol{A}^{\mathrm{T}}(\boldsymbol{S} - \boldsymbol{M})\boldsymbol{A}$ with $\boldsymbol{M} = \boldsymbol{S}^{\mathrm{T}}\boldsymbol{B}\left(\boldsymbol{R} + \boldsymbol{B}^{\mathrm{T}}\boldsymbol{S}\boldsymbol{B}\right)^{-1}\boldsymbol{B}^{\mathrm{T}}\boldsymbol{S}$. The term $\log_2|\det \boldsymbol{A}|$ is referred to as the intrinsic entropy of the controlled system, where a larger value indicates higher instability. The proposed task-oriented closed-loop scheme takes the LQR cost as the objective and takes the cycle time as the constraint. The UL and DL bandwidth, CPU frequency, and time allocation are jointly optimized. Readers can refer to Refs. [15,16] for the details of modeling methods and algorithms. In this study, we consider a static setting in which the UAV remains fixed at a given location and the channel gain is assumed to be constant, as the air-to-ground channel is dominated by the line-of-sight path. To address dynamic environments in practice, such as those with UAV movement or fluctuating channel conditions, the proposed framework needs to be implemented in a prediction-based, process-oriented manner. Techniques such as real-time radio map updates, reinforcement learning-based decision-making, and adaptive robot control can be integrated into the proposed framework to enhance adaptability.

Fig. 5(a) shows the simulation result of the single-loop optimization proposed in Ref. [15]. In this simulation, we apply the path-loss model to calculate the UL and DL channel gain ($h^{\mathrm{u/d}}$), $h^{\mathrm{u/d}}(\mathrm{dB}) = [32.4 + 20\times\log_{10}(f_{\mathrm{c}}) + 20\times\log_{10}(d^{\mathrm{u/d}})]$, where $f_{\mathrm{c}} = 2000$ (MHz) represents the carrier frequency and $d^{\mathrm{u/d}} = 1$ (km) represents the transmission distance. The transmit power for both UL and DL is set to 1 W, the communication bandwidth is $B_{\max} = 0.25$ (MHz), and the noise power spectrum density is −174 dBm. The computing-related parameters are set as follows: $f = 1$ (GHz), $\alpha = 100$ (CPU cycles per bit), and $\rho = 0.01$. The control-oriented parameters are set as: $\log_2|\det \boldsymbol{A}| = 30$, $m = 100$, $\boldsymbol{\Sigma}_{\boldsymbol{v}} = 0.01 \times \mathbf{I}_{100}$, $\boldsymbol{M} = \boldsymbol{S} = \mathbf{I}_{100}$, and $N(\boldsymbol{v}) = 0.01$, where $\mathbf{I}_{100}$ represents the 100-dimensional unit matrix. The cycle time is set as $T = 10$ (ms). We compare the proposed scheme with the communication-oriented scheme [17] and the static configuration. The scheme proposed in Ref. [17] maximizes the UL and DL sum rates, with the rate difference as a constraint. In our simulation, the rate-difference threshold is set to 100 bits per SC^3 cycle. In the static configuration, a fixed bandwidth based on the 5G FDD standard (i.e., $B^{\mathrm{u}} = B^{\mathrm{d}} = \frac{B_{\max}}{2}$, where B^{u} and B^{d} are UL bandwidth and DL bandwidth, respectively), is used, and the time allocation is set as $t^{\mathrm{u}} = \frac{1}{2}T$, $t^{\mathrm{c}} = \frac{2}{5}T$, and $t^{\mathrm{d}} = \frac{1}{10}T$, where t^{u} denotes UL transmission time and t^{d} denotes DL transmission time. Compared with 5G-based static configuration, the proposed scheme achieves a 40% reduction in the LQR cost. This is because the proposed scheme aligns UL and DL capabilities within the SC^3 loop, whereas the other two schemes fail to achieve this balance. Their bottleneck links limit the CNER, leading to poor control performance. These results validate the superiority of the task-oriented closed-loop scheme, which systematically optimizes loop components to overcome the bottleneck effect and enhance overall efficiency.

Fig. 5(b) presents the simulation result of the multi-loop optimization scheme proposed in Ref. [16]. In this simulation, we consider $K = 4$ SC^3 loops, where K denotes the loop number. Instead of calculating the channel gain as in single-loop optimization, we directly set the UL and DL spectrum efficiencies as

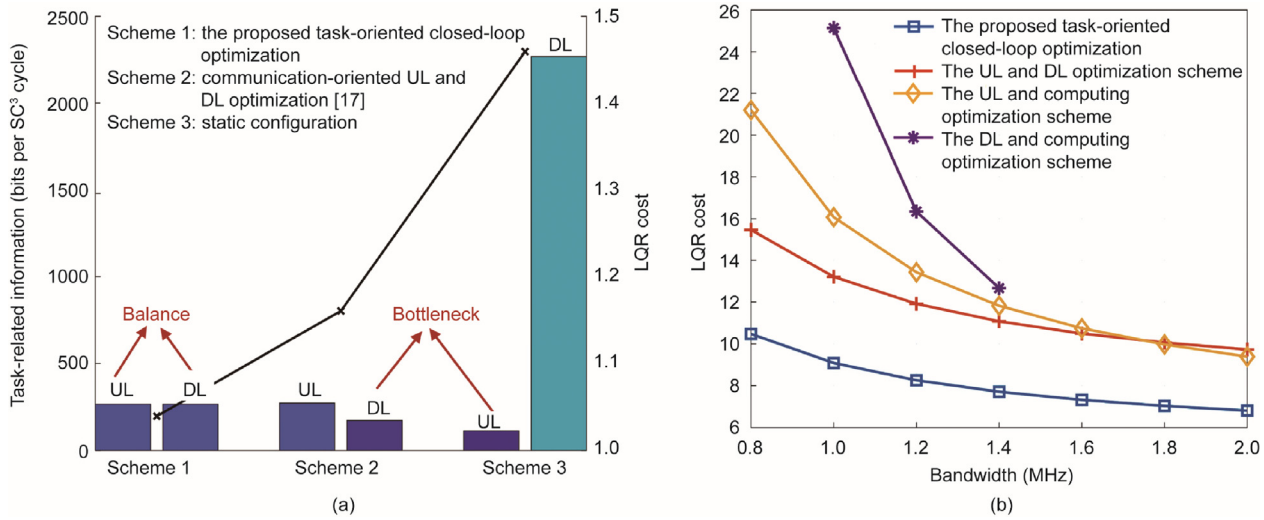

Fig. 5. (a) Simulation results for single-loop optimization. The volume of task-related information and LQR cost are presented for the proposed scheme, the communication-oriented UL and DL optimization scheme [17], and the static configuration. (b) Simulation results for multi-loop optimization. The LQR cost is presented for the proposed scheme and three modular schemes.

$r^{\mathrm{u}} = [4, 5, 6, 7]$ (bits·s^{-1}·Hz^{-1}) and $r^{\mathrm{d}} = [7, 8, 9, 10]$ (bits·s^{-1}·Hz^{-1}), respectively. In addition, the communication bandwidth ranges from 0.8 to 2 MHz, and we set $\alpha = [200, 100, 50, 500]$ (CPU cycles per bit) and $\log_2|\det \boldsymbol{A}| = [10, 10, 30, 30]$. The other parameters are consistent with those used in the single-loop optimization scheme and are the same for the SC^3 loops. We compare the proposed scheme with three modular schemes that do not perserve integrity of the SC^3 loops and only optimize parts of loop components. In the UL and DL optimization scheme, the UL and DL bandwidth and transmission time are optimized, with equally allocated CPU frequency. In the DL and computing optimization scheme, the CPU frequency and DL bandwidth and time are optimized, with the UL bandwidth $B^{\mathrm{u}} = \frac{B_{\max}}{2K}$ and time $t^{\mathrm{u}} = \frac{1}{2}T$. In the UL and computing optimization, UL bandwidth and time and CPU frequency are optimized, with the DL bandwidth $B^{\mathrm{d}} = \frac{B_{\max}}{2K}$ and time $t^{\mathrm{d}} = 1$ (ms). The three modular schemes fail to achieve control performance comparable to that of the proposed scheme. This is because their unoptimized components limit intra- and inter-loop adaptability, resulting in mismatches among the UL, computing, and DL within the SC^3 loop, as well as misaligned control progress across SC^3 loops. These results highlight the importance of treating the SC^3 loop as an integrated structure and balancing resource allocation both within and across SC^3 loops.

6. Open issues

Although the task-oriented closed-loop design clearly enables more efficient resource usage than the communication-oriented link-based design does, some theoretical and technical challenges remain. Here, we outline the related open issues and possible solutions.

6.1. Theoretical model of the SC^3 loop

In recent decades, sensing, communication, computing, and control have been developed separately. There is a lack of theoretical models that can integrate the multi-domain functions of SC^3 loops and provide a unified framework for quantifying the performance of diverse tasks. Thus, the gap between the performance in the current optimization schemes and theoretical boundaries remains unknown. We believe that extending information theory to bridge the interdependencies among the components of the SC^3 loop offers a promising direction for future research. However, a key open challenge lies in evaluating the task-specific significance of information—an aspect that goes beyond Shannon theory, in which it is assumed that all bits carry equal importance regardless of their relevance to the task [18].

6.2. Cost–benefit trade-off

The cost–benefit trade-off is critical for SAGINs and influences how environmental and task-related information is used. In addition to evaluating the benefit of the task-oriented closed-loop design, it is equally important to assess the costs associated with collecting, managing, and utilizing information. In addition, task-oriented closed-loop optimization is multi-scale, process-oriented, and space–air–ground integrated, and its complexity is much greater than that of single-scale, instant, and ground-only optimization under communication-oriented link-based schemes. Research can explore the nature of these optimization problems and develop low-complexity algorithms. In some cases, a low-cost suboptimal solution may be better than a high-cost optimal one.

6.3. Responsiveness and robustness

In addition to effectiveness, responsiveness and robustness are key dimensions of SAGINs. In disaster rescue, the network must establish SC^3 loops within seconds. This process involves hundreds of decisions, and making them at the second scale is not easy. One possible solution is to build a knowledge library that stores typical models and reusable solutions. When an emergency occurs, the network can quickly load matched responses—like a conditioned reflex arc—to take timely action. In addition, dynamic environments may cause link or device failures. To ensure service continuity, the system must rapidly reorganize new SC^3 loops. One possible solution is to design SC^3 loops with modular redundancy and partial autonomy, similar to the self-repair capability of a starfish. This allows the system to isolate and recover from local failures without impacting task execution processes.

6.4. Network analysis

The SAGIN in the considered setting is highly complex. Differences in coverage, dynamics, latency, and path loss among ground-to-ground, air-to-ground, and space-to-ground links pose considerable challenges for space–air–ground integration. In addition, different SC^3 loops involve complex coupling relationships among shared sensors, computing models, and actuators. Factors such as heterogeneity, dynamics, and complexity make analyzing entire SAGINs an arduous task. One possible approach is to focus on the basic patterns of SAGINs [19], such as the minimal structure that captures the essential differences across space, air, and ground layers and the coupled relationships among SC^3 loops. By treating the overall SAGIN as a composition and extension of these basic patterns, the analysis becomes more tractable while preserving the critical characteristics of the SAGIN.

7. Conclusions

In this work, we investigated 6G SAGINs for unmanned operations. From a systematic perspective, we treated the reflex arc-like SC^3 loop rather than the communication link as the basic unit of the SAGIN. To provide task-matched services via SC^3 loops, we devised a radio-map-based task-oriented framework, which picks up environmental and task-related information that is ignored by 5G systems. We detailed how this framework collects and uses this information and investigated task-oriented closed-loop scheduling schemes. With the control task as an example, we provided a case study to validate the superiority of the proposed task-oriented closed-loop scheme. On this basis, we have outlined open issues and possible solutions. We call for more research on task-oriented systematic design, which is promising for reforming current communication networks and developing nerve-system-like SAGINs.

CRediT authorship contribution statement

Xinran Fang: Writing – original draft, Software, Methodology, Formal analysis. **Wei Feng:** Writing – review & editing, Validation, Supervision, Resources, Project administration, Methodology, Investigation, Funding acquisition, Formal analysis. **Yunfei Chen:** Writing – review & editing, Supervision. **Ning Ge:** Supervision. **Shi Jin:** Writing – review & editing, Supervision. **Shiwen Mao:** Supervision.

Declaration of competing interest

The authors declare that they have no known competing financial interests or personal relationships that could have appeared to influence the work reported in this paper.

Acknowledgments

This work was supported in part by the National Natural Science Foundation of China (62425110 and U22A2002), the National Key Research and Development Program of China (2020YFA0711301), the Suzhou Science and Technology Project, and the FAW Jiefang Automotive Co., Ltd.

References

[1] Tseng M. Next G applications and use cases. In: Lin X, Zhang J, Liu Y, Kim J, editors. Fundamentals of 6G communications and networking. Cham: Springer; 2023. p. 93–112.
[2] Robot to remove melted nuclear fuel debris from Japan's Fukushima reactor [Internet]. Fast Company; 2024 May 29 [cited 2025 Jul 26]. Available from: https://www.fastcompany.com/91132116/robot-to-remove-melted-nuclear-fuel-debris-japans-fukushima-reactor.
[3] Saarnisaari H, Dixit S, Alouini MS, Chaoub A, Giordani M, Kliks AA. 6G white paper on connectivity for remote areas. 2020. arXiv:2004.14699.
[4] Meng S, Wu S, Zhang J, Cheng J, Zhou H, Zhang Q. Semantics-empowered space–air–ground–sea integrated network: new paradigm, frameworks, and challenges. IEEE Commun Surv Tutor 2025;27(1):140–83.
[5] Ashizawa T, Xia G. Ataxia. Continuum 2016;22(4):1208–26.
[6] Production start at Oseberg Vestflanken 2 [Internet]. Stavanger: Equinor ASA; 2018 Oct 15 [cited 2025 Jul 26]. Available from: https://www.equinor.com/news/archive/october2018-oseberg-vestflanken2.
[7] Minimize worker dose and support decommissioning efforts with spot [Internet]. Wilmington: Boston Dynamics; c2025 [cited 2025 Jul 26]. https://bostondynamics.com/solutions/safety/nuclear-decommissioning/.
[8] Feng W, Wang Y, Chen Y, Ge N, Wang CX. Structured satellite–UAV–terrestrial networks for 6G Internet of Things. IEEE Netw 2024;38(4):48–54.
[9] Fang X, Feng W, Chen Y, Ge N, Zheng G. Control-oriented deep space communications for unmanned space exploration. IEEE Trans Wirel Commun 2024;23(10):14466–81.
[10] 5G E2E technology to support verticals URLLC requirements. Frankfurt: Next Generation Mobile Networks Alliance; 2020.
[11] Zeng Y, Chen JT, Xu J, Wu D, Xu XL, Jin S. A tutorial on environment–aware communications via channel knowledge map for 6G. IEEE Commun Surv Tutor 2024;26(3):1478–519.
[12] Kostina V, Hassibi B. Rate-cost tradeoffs in control. IEEE Trans Automat Contr 2019;64(11):4525–40.
[13] Feng W, Lin Y, Wang Y, Wang J, Chen Y, Ge N. Radio map-based cognitive satellite-UAV networks towards 6G on-demand coverage. IEEE Trans Cogn Commun Netw 2024;10(3):1075–89.
[14] Fang X, Feng W, Chen Y, Yang D, Ge N, Feng Z. Radio map-based spectrum sharing for joint communication and sensing networks. IEEE Open J Commun Soc 2024;5:4541–58.
[15] Fang X, Lei C, Feng W, Chen Y, Ge N, Jin S. Structured connectivity for 6G reflex arc: task-oriented virtual user and new uplink–downlink tradeoff. IEEE Wirel Commun Lett 2025;14(1):198–202.
[16] Fang X, Lei C, Feng W, Chen Y, Xiao M, Ge N. Sensing–communication–computing–control closed-loop optimization for 6G digital twin-empowered robotic systems. IEEE J Sel Areas Commun 2025;43(10):3330–46.
[17] El-Hajj AM, Dawy Z. On optimized joint uplink/downlink resource allocation in OFDMA networks. In: Proceedings of IEEE Symposium on Computers and Communications; 2011 Jun 28–Jul 1; Kerkyra, Greece. New York City: IEEE; 2011.
[18] Li A, Wu S, Meng S, Lu R, Sun S, Zhang Q. Toward goal-oriented semantic communications: new metrics, framework, and open challenges. IEEE Wirel Commun 2024;31(5):238–45.
[19] Fang X, Feng W, Wei T, Chen Y, Ge N, Wang CX. 5G embraces satellites for 6G ubiquitous IoT: basic models for integrated satellite terrestrial networks. IEEE Internet Things J 2021;8(18):14399–417.